Cancer Biomarkers -1 (2024) 1–13 1
DOI 10.3233/CBM-230191
IOS Press

Circ_0049271 targets the *miR-1197/PTRF* axis to attenuate the malignancy of osteosarcoma

Yixin Wen[a,1], Feng Xu[b,1] and Hui Zhang[c,*]
[a]*Orthopaedics Department, Fifth Hospital in Wuhan, Wuhan, Hubei, China*
ORCID: https://orcid.org/0009-0002-1828-9458
[b]*Orthopaedics Department, Fifth Hospital in Wuhan, Wuhan, Hubei, China*
ORCID: https://orcid.org/0009-0005-1823-3819
[c]*Orthopaedics Department, Fifth Hospital in Wuhan, Wuhan, Hubei, China*
ORCID: https://orcid.org/0000-0002-5225-9167

Received 10 May 2023
Accepted 8 January 2024

Abstract.
BACKGROUND: Circular RNAs (circRNAs) perform key regulatory functions in osteosarcoma (OS) tumorigenesis. In this study, we aimed to explore the detailed action mechanisms of *circ_0049271* in OS progression.
METHODS: Cell colony formation, cell counting kit-8, and transwell assays were performed to assess the proliferation and invasion of OS cells. Quantitative reverse transcription-polymerase chain reaction and western blotting were used to determine the expression levels of polymerase 1 and transcript release factor (PTRF), microRNA (miR)-1197, and circ_0049271 in OS cells. Furthermore, RNA immunoprecipitation and dual luciferase assays were conducted to explore the targeted relationships among *PTRF*, *miR-1197*, and *circ_0049271*. Finally, a tumor formation assay was conducted to determine the effects of *circ_0049271* on *in vivo* tumor growth in mice.
RESULTS: High expression levels of *miR-1197* and low levels of *circ_0049271* and *PTRF* were observed in OS cells. *circ_0049271* targeted *miR-1197* to mediate *PTRF* expression. Moreover, the proliferation and invasion of OS cells were repressed by *circ_0049271* or *PTRF* overexpression and increased by *miR-1197* upregulation. Enforced *circ_0049271* also impeded tumor growth *in vivo*. Upregulation of *miR-1197* reversed the antitumor effects of *circ_0049271* on OS progression *in vitro*; however, *PTRF* overexpression attenuated the cancer-promoting effects of *miR-1197* on OS *in vitro*.
CONCLUSIONS: Our findings revealed that *circ_0049271* targeted the *miR-1197/PTRF* axis to attenuate the malignancy of OS, suggesting a potential target for its clinical treatment.

Keywords: Osteosarcoma, circRNA, *circ_0049271*, *miR-1197*, *PTRF*

1. Introduction

Osteosarcoma (OS) is a highly destructive bone malignancy [1]. The focal zone of OS is in the metaphysis of long bones, where active bone repair and growth occur [2]. Surgical amputation is a key treatment method for OS; however, it causes disability and leads to recurrence [3,4]. Although significant progress in chemotherapy and radiotherapy has improved the five-year survival rate to approximately 70%, adverse side effects may be observed in patients with OS [5,6,7]. Therefore, understanding the pathogenesis of OS is necessary to develop robust strategies for its treatment.

[1]The authors equally contributed to this research.
*Corresponding author: Hui Zhang, Orthopaedics Department, Fifth Hospital in Wuhan, No. 122, Xianzheng Street, Hanyang District, Wuhan 434000, Hubei, China. Tel./Fax: +86 27 84812271; E-mail: huizhang526@163.com.

Circular RNAs (circRNAs) are non-coding RNAs (ncRNAs) with a closed covalent loop structure [8,9]. Lacking 5'-caps and 3'-tails, circRNAs exhibit exonuclease resistance, making them more stable than linear RNAs [10]. The regulatory functions of circRNAs in various cancer types, including OS, have attracted attention [11,12]. For example, Yang et al. reported that patients with OS with distant metastases and large tumors exhibit high *circ_001422* expression [13]. Jiang et al. reported low levels of *circ_0000658* in OS cells and tissues [14]. Guan et al. reported that *circ_0008259* was underexpressed in OS and that its overexpression distinctly represses the metastasis and proliferation of OS cells [15]. *circ_0049271* is downregulated in non-small cell lung cancer (NSCLC), exhibiting diagnostic value in distinguishing patients with NSCLC from healthy subjects [16]. Diminished *circ_0049271* expression is closely correlated to the poor prognosis of patients with lung adenocarcinoma [17,18]. He et al. analyzed the differentially expressed circRNAs in OS and reported poor *circ_0049271* expression, suggesting its role as a tumor-suppressive circRNA in OS progression [19]. However, the specific functions and regulatory mechanisms of *circ_0049271* in OS tumorigenesis remain unclear.

MicroRNAs (miRNAs) are highly conserved ncRNAs that modulate post-transcriptional functions by binding to the 3′-untranslated region of their target mRNAs [20,21]. Recently, many studies have demonstrated the vital functions of miRNAs in the progression of OS. For example, *miR-21* is expressed at low levels in OS and is an effective biomarker for the onset of OS tumorigenesis [22]. Low *miR-505* levels have been reported in OS serum and tissues [23]. *miR-505* upregulation inhibits the proliferation and induces the apoptosis of OS cells [23]. miRNAs, such as *miR-421* [24], *miR-487a* [25], and *miR-628-5p* [26], are overexpressed in OS and considered as oncogenes for OS progression. Moreover, regulatory mechanisms of various circRNA–miRNA networks, such as *circ_0046264–miR-940* [27], *circ_0000527–miR-646* [28], and *circ_0001721–miR-372-3p* [29], have been widely investigated in the occurrence and progression of OS. *miR-1197* interacts with circRNAs in several human cancers, including *circ_0075542* in prostate cancer (PC) [30], *circ_0004018* in hepatocellular carcinoma (HCC) [31], and *circ_0000429* in NSCLC [32]. However, whether *circ_0049271* modulates the role of *miR-1197* in OS progression remains unclear.

In this study, we investigated the biological functions of *circ_0049271* in OS and explored its regulatory mechanisms *via* the *miR-1197*/polymerase 1 and transcript release factor (*PTRF*) axis. Our results highlight a promising new therapeutic target for OS treatment.

2. Methods

2.1. Sources of reagents, cells, and animals

hFOB 1.19 osteoblasts and human-derived OS cell lines (HOS and Saos-2) were purchased from Procell Life Science & Technology Co., Ltd. (Wuhan, China). Another human SW1353-derived OS cell line was provided by the BeNa Culture Collection (Beijing, China). Lipofectamine 3000, fetal bovine serum (FBS), McCoy's 5A medium, Dulbecco's Modified Eagle's Medium (DMEM), and L-15 medium were purchased from Procell Life Science & Technology Co., Ltd. Cytoplasmic and nuclear RNA purification kits were acquired from Norgen BioTek (Thorold, Canada). RNase R was purchased from Geneseed Biotech (Guangzhou, China). An RNA extraction Kit (Cwbio, Beijing, China), an Evo m-mlv reverse transcription reagent, and a SYBR green Kit (Accyrate Biology, Changsha, China) were used for quantitative reverse transcription-polymerase chain reaction (qRT-PCR). The Magna RIP RNA-Binding Protein Immunoprecipitation Kit was purchased from Millipore (Billerica, MA, USA). Cell counting kit-8 (CCK-8), crystal violet, and Matrigel were obtained from Solarbio (Beijing, China). Primary antibodies against PTRF (Cat# ab76919) and glyceraldehyde 3-phosphate dehydrogenase (GAPDH; Cat# ab8245) and horseradish peroxidase (HRP)-conjugated secondary antibodies (Cat# ab6759) for western blotting were purchased from Abcam (Cambridge, UK). Genomeditech (Shanghai, China) synthesized the pcDNA3.1-circ-circ_0049271 overexpression vector (OE-circ), pcDNA3.1-PTRF, pcDNA3.1 empty vector (OE-NC), miR-1197 mimic (mimic), and mimic-NC. Tumor xenograft models were established using four-week-old BALB/c nude mice (20–26 g) obtained from Charles River Laboratories (Sulzfeld, Germany).

2.2. Cell culture

HOS and hFOB 1.19 cells were cultivated in DMEM containing 1% penicillin/streptomycin and 10% FBS. Saos-2 cells were cultured in McCoy's 5A medium supplemented with 1% penicillin/streptomycin and 15% FBS. SW1353 cells were cultured in L-15 medium sup-

Table 1
Real-time PCR primer list

Gene		Sequences
circ_0049271	Forward	5′-AACTTCGCTGAGCAGATTGG-3′
	Reverse	5′-GCATGGGGTTCCAGAAG ATA-3′
miR-1197	Forward	5′-TCCTGGTATTTGAAGATGCGGT-3′
	Reverse	5′-AGTAGACCATGTGTCCTACGTC-3′
SPOCK1	Reverse	5′-AAAGCACAAGGCAGAAAGGA-3′
	Reverse	5′-GGGTCAAGCAGGAGGTCATA-3′
PTRF	Forward	5′-GAGCTGTTAGGACCCGATGG-3′
	Reverse	5′-CCTTCCCATTCCACTCGGAC-3′
TIMP3	Reverse	5′-AGCGCAAGGGGCTGAACTATCG-3′
	Forward	5′-CGGGTAGCCGAAATTGGAGAGC-3′
U6	Forward	5′-CTCGCTTCGGCAGCACA-3′
	Reverse	5′-AACGCTTCACGAATTTGCGT-3′
GAPDH	Forward	5′-AGAAAAACCTGCCAAATATGATGAC-3′
	Reverse	5′-TGGGTGTCGCTGTTGAAGTC-3′

plemented with 1% penicillin/streptomycin and 10% FBS. The cultures were all maintained in an incubator at 37°C with 5% CO_2. The cells were cultured until the logarithmic growth phase and then collected for subsequent experiments.

2.3. Cell transfection

Lipofectamine 3000 was used to transfect 2 μg OE-circ, 2 μg OE-PTRF, 2 μg OE-NC, 50 nM mimic, and 50 nM mimic-NC into 1×10^6 HOS and SW1353 cells when cell confluency was more than 50%. The cells were incubated for 48 h and collected for subsequent experiments.

2.4. Measurement of cell proliferation

Next, the viabilities of SW1353 and HOS cells were assessed *via* the CCK-8 assay. Briefly, 1×10^4 cells transfected with SW1353 or HOS were inoculated into a 96-well plate and incubated for 0, 24, 48, and 72 h at 37°C with 5% CO_2. Approximately 15 μL of CCK-8 solution was added to the corresponding wells, and the cells were incubated for 3 h at 37°C. OS cell viability was analyzed at 450 nm using a microplate reader (DeTie Laboratory Equipment, Nanjing, China).

Cell numbers were estimated using a cell colony experiment. HOS and SW1353 cells in a 6-well plate (3×10^2 cells/well) were incubated for two weeks. The medium was replaced every two days. Subsequently, the cells were washed, immobilized, stained, and kept at 25°C. Finally, photographs of cell colonies were captured using the Olympus light microscope (Tokyo, Japan).

2.5. Transwell invasion assay

SW1353 and HOS cells (2×10^5 cells/well) were cultured in the Matrigel-precoated upper chambers filled with DMEM without FBS. The bottom chambers were filled with DMEM with 10% FBS. After incubation for 24 h, invasive OS cells were stained with 0.5% crystal violet, and three randomly selected fields were photographed using the Olympus light microscope.

2.6. Western blotting assay

Total protein was extracted from 2×10^6 HOS and SW1352 cells after cell lysis with the radioimmunoprecipitation assay buffer, followed by total protein quantification using the BCA kit (Beyotime, China). Proteins (20 μg) were subjected to electrophoresis on a 10% sodium dodecyl sulfate-polyacrylamide gel and transferred to polyvinylidene fluoride membranes using a protein marker (10–200 kD; Beyotime). Subsequently, 5% fat-free milk was used to block the membranes, which were incubated with anti-PTRF (1:5000) and anti-GAPDH (1:2000) antibodies overnight at 4°C. Then, the membranes were incubated with HRP-conjugated secondary antibodies (1:20000) at 25°C for 2 h. An enhanced chemiluminescence detection kit (Beyotime) was used for band visualization, and GAPDH was used for normalization.

2.7. qRT-PCR

Total RNAs from OS samples and cell lines (1×10^6 cells) were isolated using an RNA extraction kit. The First-Strand cDNA Synthesis Kit was used to synthesize cDNA. PCR was performed using the Applied Biosystems (ABI) 7500 Real-Time PCR System with the SYBR Green FAST Mastermix Kit. Table 1 provides all primers used in this study based on the previous literature [33,34,35,36] and the National Center of Biotechnology Information database. Then, expres-

sion levels of *circ_0049271*, *miR-1197*, and *PTRF* were computed *via* the $2^{-\Delta\Delta Ct}$ approach. $U6$ and *GAPDH* were used for normalization.

2.8. Subcellular location analysis

The cytoplasmic and nuclear RNAs of SW1353 and HOS cells (1×10^6 cells) were separated using the Cytoplasmic and Nuclear RNA Purification Kit. Subsequently, purified RNAs were subjected to qRT-PCR. $U6$ and *GAPDH* were used as the controls for nuclei and cytoplasm, respectively.

2.9. RNase R treatment

RNAs extracted from the SW1353 and HOS cells (1×10^6 cells) were mixed with RNase R (3 U/μg) for 1 h at 37°C. Then, expression levels of *circ_0049271* and its linear gene, kelch-like ECH-associated protein 1 (*KEAP1*), were assessed *via* qRT-PCR.

2.10. RNA immunoprecipitation (RIP) assay

HOS and SW1353 cells (1×10^6 cells) were mixed with the RIP lysis buffer in a magnetic bead suspension and conjugated with anti-Ago2 or anti-IgG (5 μg/μL) overnight. After protein digestion and RNA purification, the levels of *circ_0049271*, *miR-1197*, *miR-620*, and *miR-1270* were determined *via* qRT-PCR.

2.11. Bioinformatics analysis

Two online databases, starBase (https://rnasysu.com/encori/) and CircInteractome (https://circinteractome.nia.nih.gov/index.html), were used to predict the miRNA binding to *circ_0049271*. Another database, TargetScan (https://www.targetscan.org/vert_71/), was used to predict the target genes of *miR-1197*. In addition, an mRNA microarray (GSE12865) from Gene Expression Omnibus was used to confirm the downregulated genes in OS samples with adj. $P < 0.01$ and logFC <–2. Finally, Venny 2.1.0 (https://bioinfogp.cnb.csic.es/tools/venny/) was used to overlap the common miRNAs or genes from different databases.

2.12. Dual-luciferase reporter assay

To create mutant (MUT) and wild-type (WT) *circ_0049271/PTRF*, we inserted miR-1197-binding sites on *circ_0049271/PTRF* sequences into pGL3 vectors. Recombinant vectors and mimic/mimic-NC were introduced into HOS and SW1353 cells (> 50% cell confluency). Then, the Promega Dual-Glo Luciferase Assay System (Madison, WI, USA) was used to measure the luciferase activity.

2.13. Murine xenograft model

OE-circ or OE-NC lentiviral vector was introduced into SW1353 cells (1×10^5 cells), which were subcutaneously injected into the right flank of each mouse (n = 5/group). Tumor volume was computed every four days. After four weeks, euthanasia was performed before extracting and weighing the tumor xenografts.

2.14. OS sample collection

Nineteen individuals diagnosed with OS by two pathologists using computed tomography and a surgical biopsy were enrolled in this study. Tumors and matched normal tissues (> 5 cm from the tumor) were acquired *via* surgery. The inclusion criteria for patients with OS were as follows: 1) patients initially diagnosed with OS in our hospital; 2) patients with OS who did not receive any treatment before surgery; and 3) patients who signed the informed consent forms for inclusion in this study. The exclusion criteria for patients with OS were as follows: 1) patients with recurrent OS; and 2) patients with other diseases. The collected OS specimens were stored at −80°C until use. All participants or their guardians provided written informed consent for inclusion in this study. All experimental procedures were approved by the ethics committee of the Fifth Hospital of Wuhan (approval number: 2022-11-07).

2.15. Statistical analyses

Data are represented as the mean ± standard deviation. All data were analyzed using the SPSS v.22.0 software. Pearson's correlation coefficient was used for linear correlation analysis. Differences between groups were analyzed using the Student's t-test. In contrast, those among more than two groups were analyzed using the analysis of variance followed by Tukey's post-hoc or Sidak's multiple comparisons tests. Statistical significance was set at $P < 0.05$.

3. Results

3.1. Circ_0049271 is underexpressed in OS

Here, *circ_0049271* expression levels were considerably lower in tumor tissues than in the corresponding normal tissues (Fig. 1A). Moreover, *circ_0049271* was underexpressed in SW1353, HOS, and Saos-2 OS cells relative to its expression in hFOB1.19 cells (Fig. 1B).

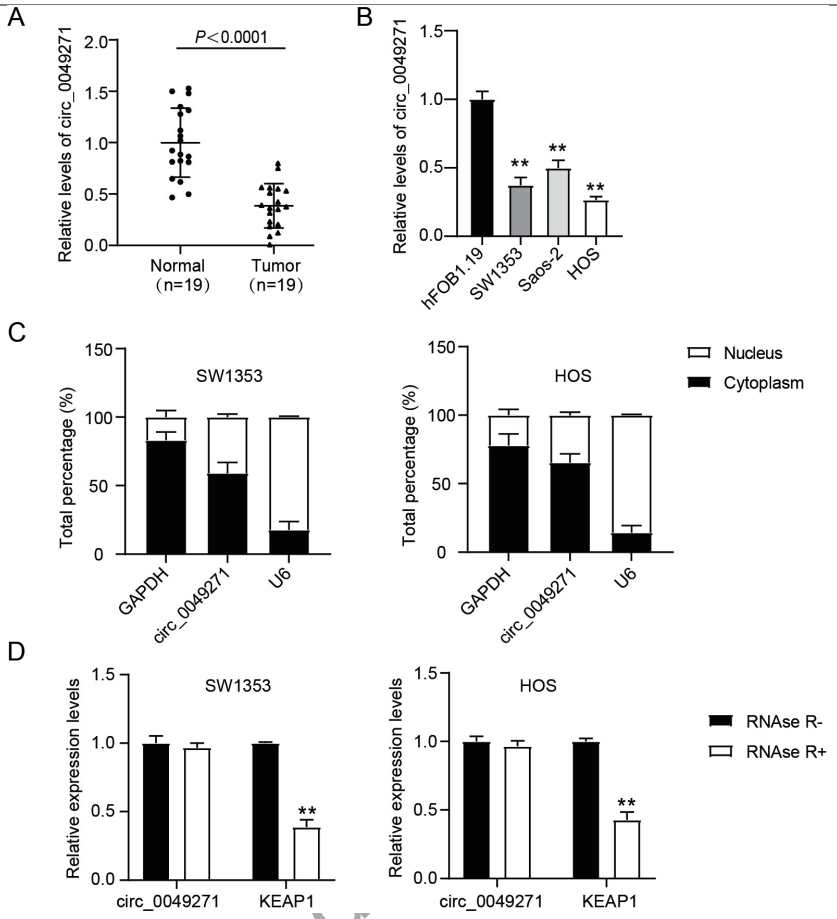

Fig. 1. Circ_0049271 is under-expressed in OS. (A) Circ_0049271 levels in OS normal and tumoral tissues were estimated through qRT-PCR. $P <$ 0.0001 vs. normal. (B) Circ_0049271 levels in hFOB1.19 cells and OS cell lines were quantified through qRT-PCR. $^{**}P < 0.01$ vs. hFOB1.19 cells. (C) Relative circ_0049271 expressions within the nuclei and cytoplasm of SW1353 and HOS cells as quantified through subcellular localization analysis. (D) The levels of circ_0049271 and the corresponding linear KEAP1 in total cellular RNA incubated with RNase R. $^{**}P <$ 0.01 vs. control.

Therefore, SW1353 and HOS cells were selected for subsequent experiments. A subcellular localization assay revealed that circ_0049271 was mainly localized in the cytoplasm (Fig. 1C). To corroborate its circular features, *circ_0049271* and its linear transcript, *KEAP1*, were treated with RNase R. As shown in Fig. 1D, unlike *KEAP1*, *circ_0049271* exhibited resistance to RNase R digestion. These findings suggest that *circ_0049271* is underexpressed and functions as a competing endogenous RNA (ceRNA) in OS.

3.2. Enforced circ_0049271 suppresses the invasion and proliferation of OS cells in vitro and tumor growth in vivo

To verify the effects of *circ_0049271* on OS cells, it was overexpressed by transfecting SW1353 and HOS cells with OE-circ (Fig. 2A). As shown in Fig. 2B, the viability of OS cells decreased markedly after *circ_0049271* overexpression. Moreover, *circ_0049271* overexpression reduced the number of OS cell colonies (Fig. 2C) and suppressed the invasion of SW1353 and HOS cells (Fig. 2D). In addition, analysis of the influence of *circ_0049271* on solid tumor growth revealed that the injection of stably overexpressing *circ_0049271* drastically diminished the tumor volume and weight in SW1353 cells (Fig. 2E). Therefore, *circ_0049271* represses OS tumorigenesis *in vivo* and *in vitro*.

3.3. Circ_0049271 binds to miR-1197

To confirm miRNA binding to *circ_0049271*, starBase and circInteractome databases were used to predict the binding of three miRNAs (*miR-1197*, *miR-620*,

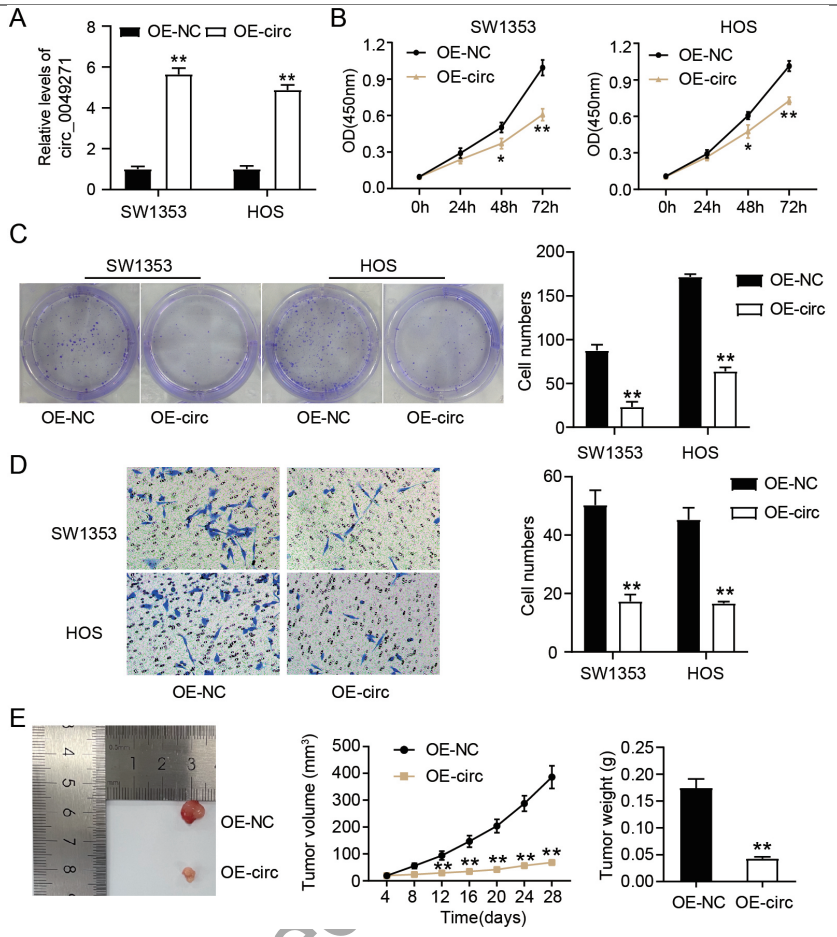

Fig. 2. Enforced circ_0049271 suppresses the invasion and proliferation of OS cells *in vitro* as well as the growth of tumors *in vivo*. (A) Circ_0049271 levels in HOS and SW1353, following their OE-circ/NC transfection, were estimated through quantitative RT-PCR. $^{**}P < 0.01$ vs. OE-NC. The viability (B) and colony numbers (C) of SW1353 and HOS cells harboring either OE-circ/NC were assessed through the CCK-8 and colony formation experiments. $^{*}P < 0.05$, $^{**}P < 0.01$ vs. OE-NC. (D) The invasive capacity of SW1353 and HOS as assessed in the transwell experiment. $^{**}P < 0.01$ vs OE-NC. (E) Representative image, volume, and weight of xenograft tumors after injecting the mice with SW1353 cells stably expressing OE-circ/NC. $^{**}P < 0.01$ vs. OE-NC.

and *miR-1270*) to *circ_0049271* (Fig. 3A). RIP assays of SW1353 and HOS cells revealed that, compared to *miR-620* and *miR-1270*, *circ_0049271* and *miR-1197* were principally enriched by Ago2 antibodies (Fig. 3B). As shown in Fig. 3C, the circInteractome revealed binding sites between *circ_0049271* and *miR-1197*. Moreover, the luciferase reporter assay indicated no obvious changes in the luciferase activity of the circ_0049271 MUT plus mimic and circ_0049271 MUT plus mimic-NC groups. Luciferase activity in the circ_0049271 WT plus mimic group was significantly lower than that in the circ_0049271 WT plus mimic-NC group (Fig. 3D). Relative to the respective NCs, elevated levels of *miR-119* were detected in OS tissues (Fig. 3E) and cell lines (Fig. 3F). *Circ_0049271* expression exhibited an inverse linear correlation with *miR-1197* expression in OS tissues (Fig. 3G). Mimic/mimic-NC was introduced into SW1353 and HOS cells to verify this regulatory relationship. As illustrated in Fig. 3H, *miR-1197* expression levels increased after mimic transfection and decreased after OE-circ transfection. Furthermore, transfection with a mimic partially attenuated the repressive effect of OE-circ on *miR-1197* expression. Therefore, *circ_0049271* targets *miR-1197,* and these two exhibit a negative regulatory relationship with each other in OS.

3.4. *Circ_0049271 overexpression abates the proliferation and invasion of OS cells via miR-1197 modulation*

Rescue experiments investigated the interaction between *circ_0049271* and *miR-1197* in SW1353 and

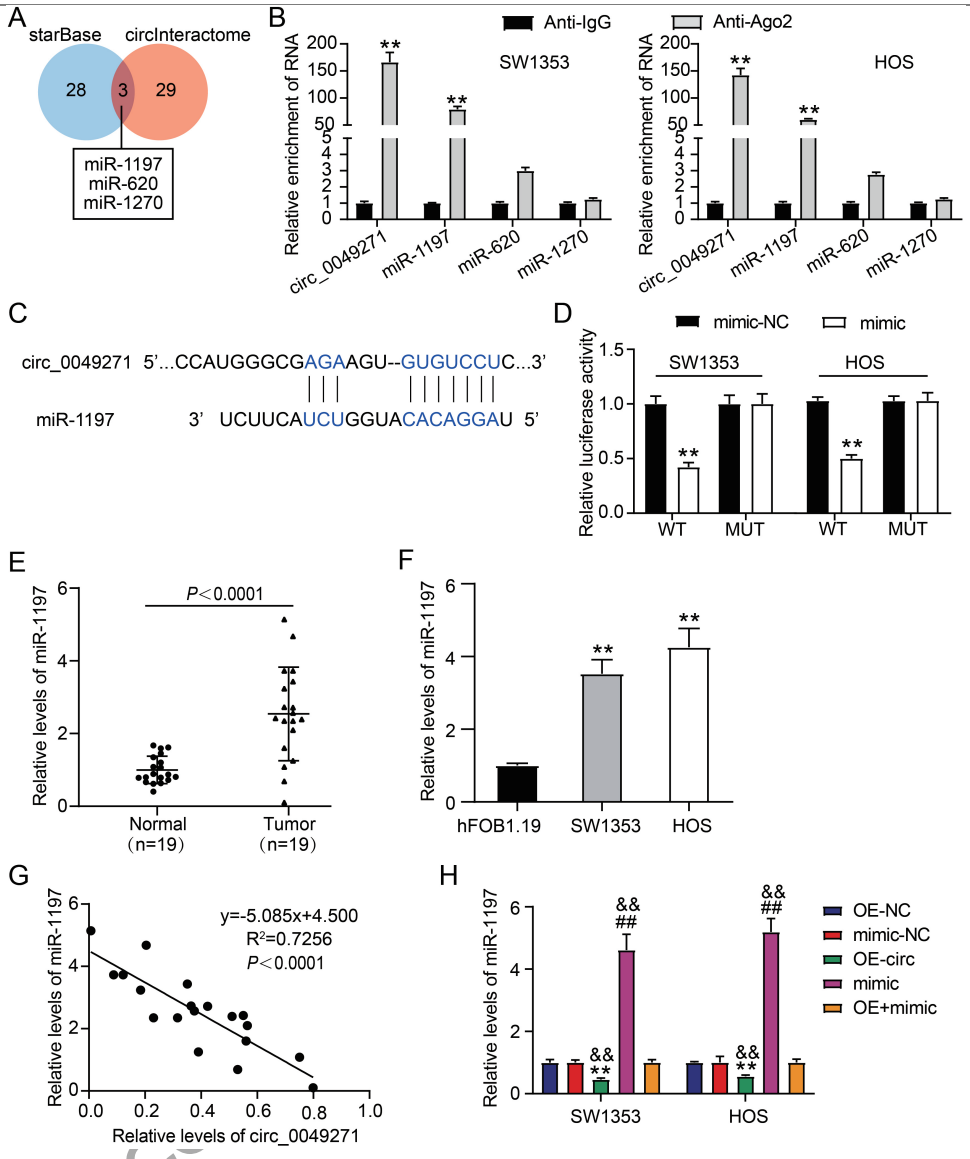

Fig. 3. Circ_0049271 binds to miR-1197. (A) starBase and circInteractome predicted the miRNAs binding to circ_0049271. (B) RIP experiment was accomplished to verify the interaction of miR-1197/miR-620/miR-1270 with circ_0049271. $^{**}P < 0.01$ vs Anti-IgG. (C) The binding sites between miR-1197 and circ_0049271. (D) The luciferase activities in HOS and SW1353 transfected with a combination of a pGL3-circ_0049271 WT/MUT and either a miR-1197 mimic/NC were gauged through the dual luciferase experiment. $^{**}P < 0.01$ vs. circ_0049271 WT + mimic-NC. (E) The miR-1197 levels in OS normal and tumoral tissues were analyzed *via* quantitative RT-PCR. $P < 0.0001$ vs. normal. (F) MiR-1197 levels in hFOB1.19 cells and OS cell lines were estimated through quantitative RT-PCR. $^{**}P < 0.01$ vs hFOB1.19 cells. (G) The correlation of miR-1197 expression with that of circ_0049271 in OS tissues was ascertained through the Pearson correlation coefficient. (H) MiR-1197 expression in SW1353 and HOS cells, after their OE-circ, OE-NC, mimic, mimic-NC, or OE-circ + mimic transfection, were quantified *via* qRT-PCR. $^{**}P < 0.01$ vs. OE-NC. $^{\#\#}P < 0.01$ vs. mimic-NC. $^{\&\&}P < 0.01$ vs. OE-circ + mimic.

HOS cells. Overexpression of *miR-1197* distinctly enhanced the viability (Fig. 4A), number (Fig. 4B), and invasion (Fig. 4C) of SW1353 and HOS cells. Impaired proliferation and invasion of OS cells caused by enforced *circ_0049271* were considerably reversed by *miR-1197* upregulation (Fig. 4A–C). These findings imply that *circ_0049271* acts as a ceRNA of *miR-1197* in OS progression.

3.5. *PTRF is a target of miR-1197*

TargetScan was used to identify the target genes of *miR-1197*. An mRNA microarray (GSE12865) was

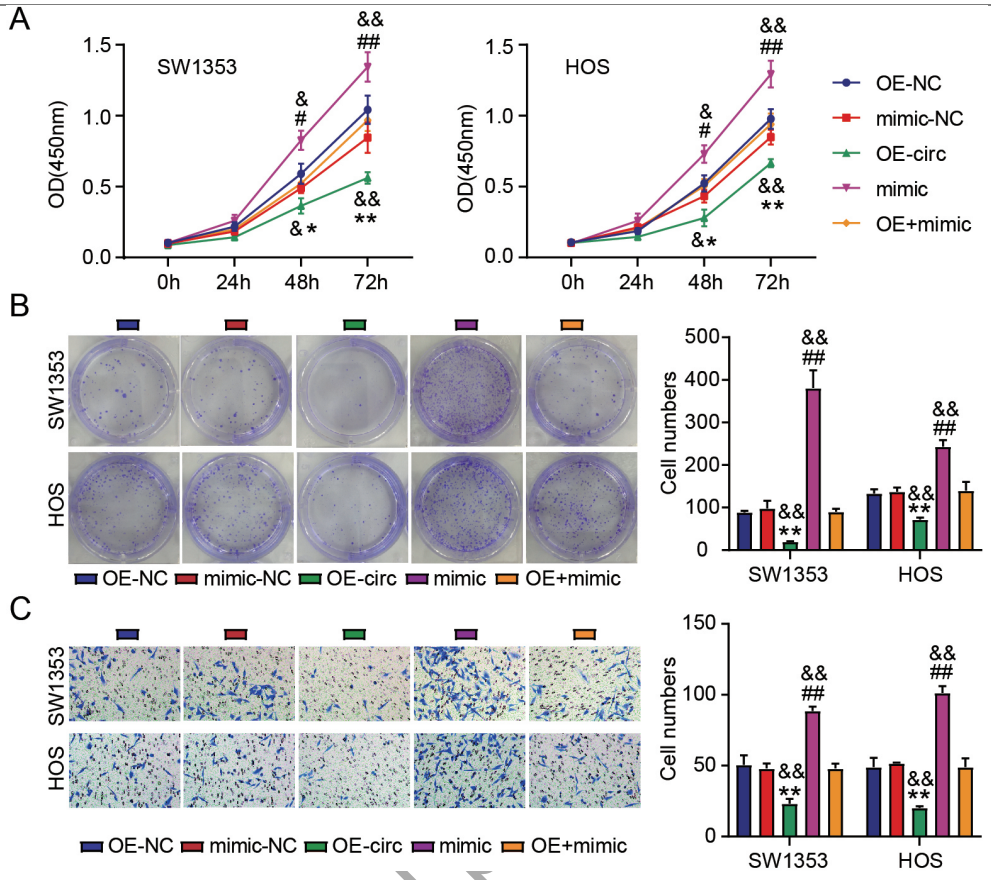

Fig. 4. Circ_0049271 overexpression prohibits the invasion and proliferation of cells through miR-1197 modulation in OS. The viability (A) and colony numbers (B) of SW1353 and HOS cells transfected with OE-circ, OE-NC, mimic, mimic-NC, or OE-circ + mimic were measured by means of the CCK-8 and colony formation experiments. (C) SW1353 and HOS cell invasion was evaluated through the transwell experiment. $^{\#}P < 0.05$; $^{\#\#}P < 0.01$ vs. mimic-NC. $^{\&}P < 0.05$; $^{\&\&}P < 0.01$ vs. OE-circ + mimic. $^{*}P < 0.05$; $^{**}P < 0.01$ vs. OE-NC.

used to identify the downregulated genes in OS samples. Using Venny 2.1.0, three genes (*SPOCK1*, *PTRF*, and tissue inhibitor of metalloproteinase 3 [*TIMP3*]) overlapped between the TargetScan and GSE12865 datasets (Fig. 5A). qRT-PCR revealed that only *PTRF* expression was reduced and inversely correlated with *miR-1197* expression in OS tissues (Fig. 5B–C). Therefore, PTRF was selected for further investigation. Figure 5D shows the TargetScan-predicted binding site of *miR-1197* on *PTRF*. Luciferase reporter assays revealed that combining PTRF WT and mimic markedly diminished the luciferase activity in SW1353 and HOS cells. However, luciferase activity was barely affected by the combination of *PTRF* MUT and mimic or mimic-NC (Fig. 5E). Reduced *PTRF* expression was detected in OS cell lines (Fig. 5F). Western blotting revealed that OE-PTRF transfection markedly elevated PTRF protein levels. In contrast, mimic transfection reduced PTRF production in SW1353 and HOS cells (Fig. 5G). Moreover, decreased PTRF protein levels *via* mimic transfection were reversed by transfecting OE-PTRF into SW1353 and HOS cells (Fig. 5G). These data suggest that *miR-1197* targets *PTRF* and inversely modulates its expression.

3.6. *miR-1197/PTRF axis is associated with the proliferation and invasion of OS cells*

Next, the interaction between *miR-1197* and *PTRF* during OS progression was verified *in vitro*. High levels of *PTRF* decreased the viability (Fig. 6A) and colony number (Fig. 6B) of OS cells. Moreover, *PTRF* overexpression inhibited OS cell invasion (Fig. 6C). *PTRF* overexpression further attenuated the promotive effect of *miR-1197* upregulation on the proliferation and invasion of OS cells (Fig. 6A–C). Our data suggest that *miR-1197* interacts with *PTRF* during OS progression.

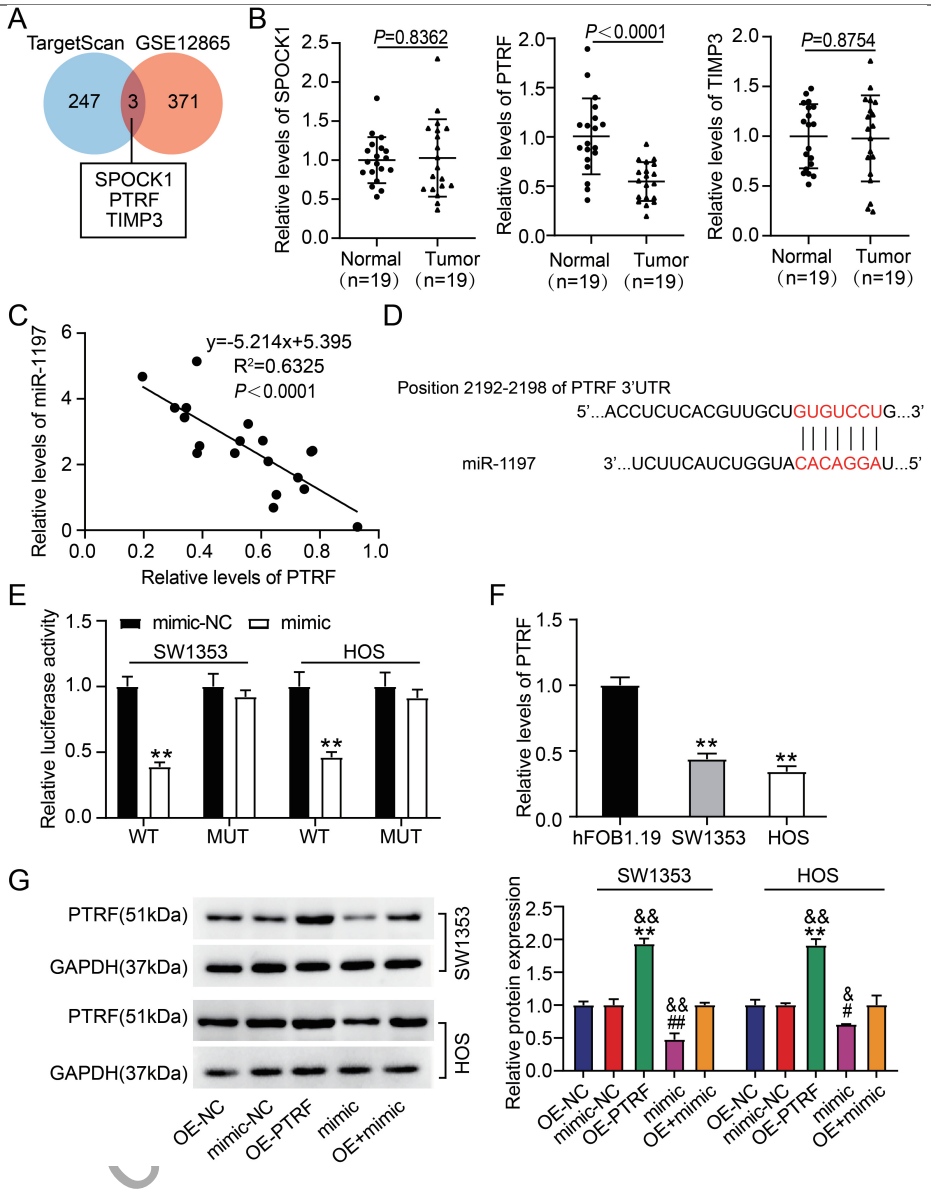

Fig. 5. MiR-1197 targets *PTRF*. (A) Three genes were overlapped from TargetScan and GSE12865. (B) The levels of *SPOCK1, PTRF, and TIMP3* in OS normal and tumoral tissues were estimated *via* quantitative RT-PCR. $P < 0.0001$ vs. normal. (C) The correlation between the miR-1197 and *PTRF* expressions in OS tissues was ascertained through Pearson correlation coefficient. (D) TargetScan predicted a miR-1197 – *PTRF* binding site. (E) The target relationship of miR-1197 with *PTRF* was verified through the dual luciferase experiment. $^{**}P < 0.01$ vs PTRF WT + mimic-NC. (F) *PTRF* levels in hFOB1.19 cells and OS cell lines were gauged through qRT-PCR. $^{**}P < 0.01$ vs. hFOB1.19 cells. (G) The levels of PTRF proteins in HOS and SW1353, after their OE-PTRF, OE-NC, mimic, mimic-NC, or OE-PTRF + mimic transfection, were analyzed *via* western blotting. $^{\#}P < 0.05$, $^{\#\#}P < 0.01$ vs. mimic-NC. $^{**}P < 0.01$ vs. OE-NC. $^{\&}P < 0.05$, $^{\&\&}P < 0.01$ vs. OE-PTRF + mimic.

4. Discussion

OS is a malignant bone tumor that originates from bone mesenchymal stem cell lesions [37,38]. Identification of effective approaches to prevent metastasis and excessive growth is important for the clinical treatment of OS. Our data revealed that *circ_0049271* expression was reduced in OS and that its overexpression attenuated OS tumorigenesis. In addition, *circ_0049271* prevented OS progression by interacting with the *miR-1197/PTRF* axis.

Various circRNAs, such as *circ_0000190* and *circ_0008259* [15,39], are aberrantly expressed in OS. They are downregulated in OS tissues and are regarded

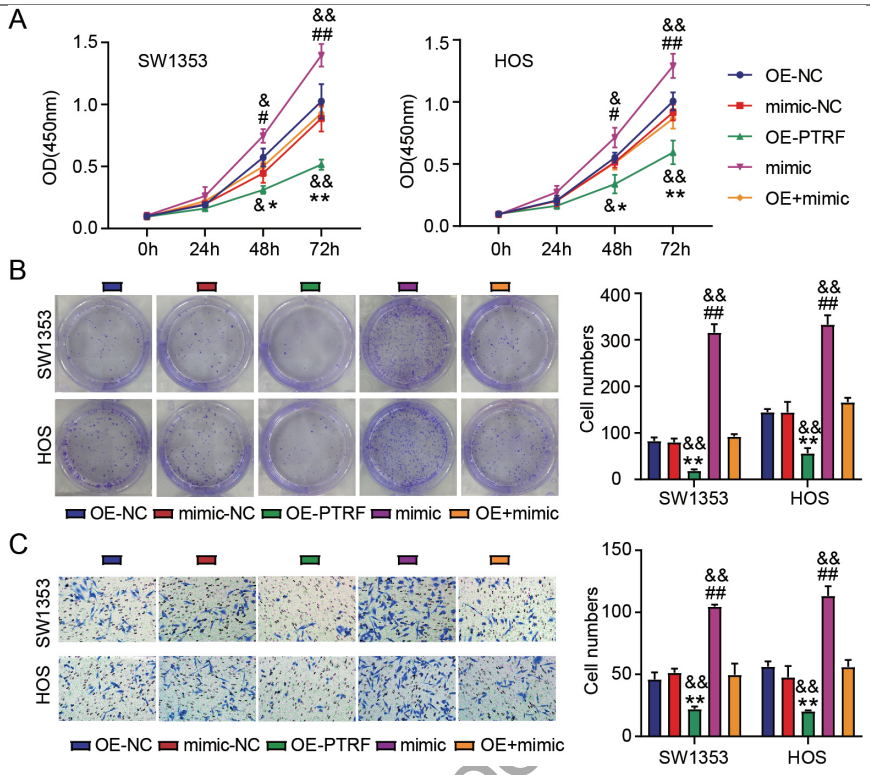

Fig. 6. MiR-1197/*PTRF* axis is associated with the abilities of OS cells to invade and proliferate. The viability (A) and colony numbers (B) of SW1353 and HOS cells carrying OE-PTRF, OE-NC, mimic, mimic-NC, or OE-PTRF + mimic were evaluated through the CCK-8 and colony formation experiments. (C) SW1353 and HOS cell invasion was assessed by means of the transwell experiment. $^{\#}P < 0.05$, $^{\#\#}P < 0.01$ vs. mimic-NC. $^{*}P < 0.05$, $^{**}P < 0.01$ vs. OE-NC. $^{\&}P < 0.05$, $^{\&\&}P < 0.01$ vs. OE-PTRF + mimic.

as inhibitors of OS progression [15,39]. In contrast, *circ_0010220* and *circ_0032462* are overexpressed and act as oncogenes during OS tumorigenesis [40,41]. The data in this study indicate that *circ_0049271* is underexpressed in OS cells and tissues. Our results lend credence to an earlier study by He et al., wherein they performed bioinformatics analyses to detect low *circ_0049271* expression in OS [19]. In our study, we pointed out that overexpression of *circ_0049271* exerted repressive effects on cell invasion and proliferation. Moreover, we discovered that the upregulation of circ_0049271 hindered tumor growth in a mouse model. These results suggest that *circ_0049271* may function as an anticancer circRNA in OS by suppressing cell invasion and growth.

Many studies have shown that *miR-1197* has various regulatory functions in human cancers. For example, *miR-1197* overexpression, which plays an important role in the tumorigenicity of the two cancers, has been observed in PC and HCC [30,31]. However, in the tumorigenesis of NSCLC, low expression levels of *miR-1197* have been detected during NSCLC tumorigenesis [32,42]. In this study, we observed elevated miR-1197 levels in OS cells and tissues. This suggests that *miR-1197* may be a risk factor for expediting the carcinogenicity of OS cells. CircRNA–miRNA crosstalk has crucial regulatory effects on the onset and development of OS [27,28,29]. miR-1197 has been confirmed to be modulated by *circ_0075542* [30], *circ_0004018* [31], and *circ_0000429* [32] to affect the progression of various cancers except for OS. Therefore, we speculated that *miR-1197* may be correlated with *circ_0049271* in OS progression. CircInteractome revealed a circ_0049271–miR-1197 binding site, implying that *miR-1197* is a downstream target of *circ_0049271*. To a certain extent, this result substantiates our hypothesis. Further rescue experiments revealed that overexpression of *miR-1197* reversed the inhibitory effects of *circ_0049271* upregulation on the invasive and proliferative potential of OS cells to a great extent. This finding supports the aforementioned hypothesis. Hence, we suggest that circ_0049271–miR-1197 crosstalk attenuates the malignancy of OS.

PTRF, named cavin-1, partakes in cellular processes by acting as a membrane sensor [43]. However, the

specific role of *PTRF* in cancer progression remains unclear. Multiple studies suggest that *PTRF* serves as a tumor inhibitor, as its underexpression is accompanied by the development of breast [44] and lung [45] cancers. In contrast, recent studies have reported its cancer-promoting roles in glioma and pancreatic cancer [46, 47]. This study detected poor PTRF expression in OS cells and tissues. A recent study by Huertas-Martínez et al. revealed poor expression of *PTRF* in Ewing sarcoma, a type of primary bone tumor mainly occurring in adolescents [48]. These findings suggest that *PTRF* is a tumor-suppressive gene in OS. Additionally, recent investigations have shown that the circRNA–miRNA–mRNA network may be an efficacious treatment option for patients with OS [19,49]. Based on the data obtained from our study, *PTRF* was hypothesized to be modulated by the circ_0049271–miR-1197 axis, which influences OS progression. In this study, *PTRF* was verified as the target gene of *miR-1197*, suggesting its interaction with *miR-1197* to mediate OS tumorigenicity. As shown in Fig. 6, overexpression of *PTRF* drastically attenuated the proliferation and invasion of cells, which were promoted by *miR-1197* upregulation. These data indicate that *circ_0049271* impedes the malignancy of OS by repressing cell invasion and proliferation *via* the *miR-1197/PTRF* axis.

This study has certain limitations. *PTRF* is a conserved cytoplasmic protein that exerts its functions *via* exosome secretion [50,51]. In OS progression, whether *PTRF* directly interacts with the *circ_0049271/miR-1197* axis or indirectly *via* exosome secretion warrants further investigation. Moreover, the impact of the *circ_0049271/miR-1197/PTRF* regulatory axis on tumor growth *in vivo* needs to be explored further in future studies.

5. Conclusion

To the best of our knowledge, this study is the first to demonstrate that *circ_0049271* attenuates the malignancy of OS *via* the *miR-1197/PTRF* axis. Our findings suggest that *circ_0049271* acts as a tumor-suppressive circRNA in OS progression. Moreover, our results reveal a novel regulatory network underlying the pathogenesis of OS and suggest a potential target for its treatment.

Funding

This work was supported by Wuhan Medical Research Project under the project name of "Experimental study of nano-hydroxyapatite/β-tricalcium phosphate loaded with cationic liposomal vancomycin in the treatment of chronic osteomyelitis in rabbits". [Grant number: WX19Y14].

Conflict of interest

The authors have declared that there were no conflicts of interest.

Ethics approval

This research received approval from the ethics committee of Fifth hospital in Wuhan (Wuhan, China). The handling of the clinical tissue specimens complied with the Declaration of Helsinki's ethical precepts. An informed consent form was completed by each patient.

The ethical use of animals has been granted by the Ethics Committee of Fifth hospital in Wuhan (Wuhan, China). Animal experiments were executed in strict accordance with the ARRIVE guidelines.

Consent to participate

All patients submitted an informed consent form.

Consent for publication

The participants provided their consent for the publication of this study.

Availability of data and material

This article includes all of the data that were gathered or examined during this investigation.

Authors' contributions

Conception: YXW and FX.
Interpretation or analysis of data: HZ and YXW.
Preparation of the manuscript: YXW and FX.
Revision for important intellectual content: YXW, FX and HZ.
Supervision: all authors.
This manuscript has been reviewed and approved by all authors.

Acknowledgments

None.

References

[1] M.S. Isakoff, S.S. Bielack, P. Meltzer and R. Gorlick, Osteosarcoma: Current Treatment and a Collaborative Pathway to Success, *J Clin Oncol* **27**(33) (2015), 3029–35.

[2] G. Ottaviani and N. Jaffe, The epidemiology of osteosarcoma, *Cancer Treat Res*, (152) (2009), 3–13.

[3] J.L. Ferguson and S.P. Turner, Bone Cancer: Diagnosis and Treatment Principles, *Am Fam Physician* **4**(98) (2018), 205–13.

[4] S.C. Kaste, C.B. Pratt, A.M. Cain, D.J. Jones-Wallace and B.N. Rao, Metastases detected at the time of diagnosis of primary pediatric extremity osteosarcoma at diagnosis: imaging features, *Cancer* **8**(86) (1999), 1602–8.

[5] E. Simpson and H.L. Brown, Understanding osteosarcomas, *Jaapa* **8**(31) (2018), 15–9.

[6] C. Zhou, W. Tan, H. Lv, F. Gao and J. Sun, Hypoxia-inducible microRNA-488 regulates apoptosis by targeting Bim in osteosarcoma, *Cell Oncol (Dordr)* **5**(39) (2016), 463–71.

[7] G.A. Marulanda, E.R. Henderson, D.A. Johnson, G.D. Letson and D. Cheong, Orthopedic surgery options for the treatment of primary osteosarcoma, *Cancer Control* **1**(15) (2008), 13–20.

[8] G. Lu, J. Zhang, X. Liu, W. Liu, G. Cao, C. Lv, et al. Regulatory network of two circRNAs and an miRNA with their targeted genes under astilbin treatment in pulmonary fibrosis, *J Cell Mol Med* **10**(23) (2019), 6720–9.

[9] H. Bai, K. Lei, F. Huang, Z. Jiang and X. Zhou, Exo-circRNAs: a new paradigm for anticancer therapy, *Mol Cancer* **1**(18) (2019), 56.

[10] J. Li, J. Yang, P. Zhou, Y. Le, C. Zhou, S. Wang, et al. Circular RNAs in cancer: novel insights into origins, properties, functions and implications, *Am J Cancer Res* **2**(5) (2015), 472–80.

[11] Z. Li, X. Li, D. Xu, X. Chen, S. Li, L. Zhang et al., An update on the roles of circular RNAs in osteosarcoma, *Cell Prolif* **1**(54) (2021), e12936.

[12] Y. Xi, M. Fowdur, Y. Liu, H. Wu, M. He and J. Zhao, Differential expression and bioinformatics analysis of circRNA in osteosarcoma, *Biosci Rep* **5**(39) (2019).

[13] B. Yang, L. Li, G. Tong, Z. Zeng, J. Tan, Z. Su, et al., Circular RNA circ_001422 promotes the progression and metastasis of osteosarcoma via the miR-195-5p/FGF2/PI3K/Akt axis, *J Exp Clin Cancer Res* **1**(40) (2021), 235.

[14] X. Jiang and D. Chen, Circular RNA hsa_circ_0000658 inhibits osteosarcoma cell proliferation and migration via the miR-1227/IRF2 axis, *J Cell Mol Med* **1**(25) (2021), 510–20.

[15] K. Guan, S. Liu, K. Duan, X. Zhang, H. Liu, B. Xu, et al., Hsa_circ_0008259 modulates miR-21-5p and PDCD4 expression to restrain osteosarcoma progression, *Aging (Albany NY)* **23**(13) (2021), 25484–95.

[16] L. Li, D. Sun, X. Li, B. Yang and W. Zhang, Identification of Key circRNAs in Non-Small Cell Lung Cancer, *Am J Med Sci* **1**(361) (2021), 98–105.

[17] L. Gao and L. Zhang, Construction and comprehensive analysis of a ceRNA network to reveal potential prognostic biomarkers for lung adenocarcinoma, *BMC Cancer* **1**(21) (2021), 849.

[18] Y. Liu, X. Wang, L. Bi, H. Huo, S. Yan, Y. Cui, et al., Identification of Differentially Expressed Circular RNAs as miRNA Sponges in Lung Adenocarcinoma, *J Oncol*, (10) (2021), 5193913.

[19] Y. He, H. Zhou, W. Wang, H. Xu and H. Cheng, Construction of a circRNA-miRNA-mRNA Regulatory Network Reveals Potential Mechanism and Treatment Options for Osteosarcoma, *Front Genet*, (12) (2021), 632359.

[20] A.C. Panda, Circular RNAs Act as miRNA Sponges, *Advances in Experimental Medicine and Biology*, (1087) (2018), 67–79.

[21] E. Anastasiadou, L.S. Jacob and F.J. Slack, Non-coding RNA networks in cancer, *Nat Rev Cancer* **1**(18) (2018), 5–18.

[22] S. Wang, F. Ma, Y. Feng, T. Liu and S. He, Role of exosomal miR21 in the tumor microenvironment and osteosarcoma tumorigenesis and progression (Review), *Int J Oncol* **5**(56) (2020), 1055–63.

[23] G. Li, F. Liu, J. Miao and Y. Hu, miR-505 inhibits proliferation of osteosarcoma via HMGB1, *FEBS Open Bio* **7**(10) (2020), 1251–60.

[24] Z. Ren, M. He, T. Shen, K. Wang, Q. Meng, X. Chen et al., MiR-421 promotes the development of osteosarcoma by regulating MCPIP1 expression, *Cancer Biol Ther* **3**(21) (2020), 231–40.

[25] Z. Gu, S. Wu, G. Xu, W. Wu, B. Mao and S. Zhao, miR-487a performs oncogenic functions in osteosarcoma by targeting BTG2 mRNA, *Acta Biochim Biophys Sin (Shanghai)* **6**(52) (2020), 631–7.

[26] J. Wang, Z. Li, X. Wang, Y. Ding and N. Li, The tumor suppressive effect of long non-coding RNA FRMD6-AS2 in uteri corpus endometrial carcinoma, *Life Sciences*, (243) (2020), 117254.

[27] R. Du, B. Fu, G. Sun, B. Ma, M. Deng, X. Zhu et al., Circular RNA circ_0046264 Suppresses Osteosarcoma Progression via microRNA-940/Secreted Frizzled Related Protein 1 Axis, *Tohoku J Exp Med* **3**(254) (2021), 189–97.

[28] X. Wu, L. Yan, Y. Liu and L. Shang, Circ_0000527 promotes osteosarcoma cell progression through modulating miR-646/ARL2 axis, *Aging (Albany NY)* **4**(13) (2021), 6091–102.

[29] Y. Gao, H. Ma, Y. Gao, K. Tao, L. Fu, R. Ren et al., CircRNA Circ_0001721 Promotes the Progression of Osteosarcoma Through miR-372-3p/MAPK7 Axis, *Cancer Manag Res*, (12) (2020), 8287–302.

[30] Y. Han, X. Wen, X. Li, D. Chen, L. Peng, B. Lai et al., Circular RNA hsa_circ_0075542 acts as a sponge for microRNA-1197 to suppress malignant characteristics and promote apoptosis in prostate cancer cells, *Bioengineered* **1**(12) (2021), 5620–31.

[31] H. Wang, Q. Zhang, W. Cui, W. Li and J. Zhang, Circ_0004018 suppresses cell proliferation and migration in hepatocellular carcinoma via miR-1197/PTEN/PI3K/AKT signaling pathway, *Cell Cycle* **20**(20) (2021), 2125–36.

[32] J.Y. Wang, F. Zhang, L. Hong and S.J. Wei, CircRNA_0000429 Regulates Development of NSCLC by Acting as a Sponge of miR-1197 to Control MADD, *Cancer Manag Res*, (13) (2021), 861–70.

[33] Y. Li, R. Shi, G. Zhu, C. Chen, H. Huang, M. Gao et al., Construction of a circular RNA-microRNA-messenger RNA regulatory network of hsa_circ_0043256 in lung cancer by integrated analysis, *Thoracic Cancer* **1**(13) (2022), 61–75.

[34] B. Zhang, W. Guo, C. Sun, H.Q. Duan, B.B. Yu, K. Mu et al., Dysregulated MiR-3150a-3p Promotes Lumbar Intervertebral Disc Degeneration by Targeting Aggrecan, *Cellular Physiology and Biochemistry: International Journal of Experimental Cellular Physiology, Biochemistry, And Pharmacology* **6**(45) (2018), 2506–15.

[35] V.L. Veenstra, H. Damhofer, C. Waasdorp, A. Steins, H.M. Kocher, J.P. Medema et al., Stromal SPOCK1 supports invasive

pancreatic cancer growth, *Molecular Oncology* **8**(11) (2017), 1050–64.

[36] Y. Gao, T. Zou, W. Liang, Z. Zhang and M. Qie, Long non-coding RNA HAND2-AS1 delays cervical cancer progression via its regulation on the microRNA-21-5p/TIMP3/VEGFA axis, *Cancer Gene Therapy* **6**(28) (2021), 619–33.

[37] J. Ritter and S.S. Bielack, Osteosarcoma. Ann Oncol. (21 Suppl 7) (2010), vii320–5.

[38] C.A. Arndt, P.S. Rose, A.L. Folpe and N.N. Laack, Common musculoskeletal tumors of childhood and adolescence, *Mayo Clin Proc* **5**(87) (2012), 475–87.

[39] S. Li, Y. Pei, W. Wang, F. Liu, K. Zheng and X. Zhang, Extracellular nanovesicles-transmitted circular RNA has_circ_0000190 suppresses osteosarcoma progression, *J Cell Mol Med* **3**(24) (2020), 2202–14.

[40] Z. Lu, C. Wang, X. Lv and W. Dai, Hsa_circ_0010220 regulates miR-198/Syntaxin 6 axis to promote osteosarcoma progression, *J Bone Oncol*, (28) (2021), 100360.

[41] R. Gu, X. Li, X. Yan, Z. Feng and A. Hu, Circular RNA circ_0032462 Enhances Osteosarcoma Cell Progression by Promoting KIF3B Expression, *Technol Cancer Res Treat*, (19) (2020), 1533033820943217.

[42] B. Sun, J. Hua, H. Cui, H. Liu, K. Zhang and H. Zhou, MicroRNA-1197 downregulation inhibits proliferation and migration in human non-small cell lung cancer cells by upregulating HOXC11, *Biomed Pharmacother*, (117) (2019), 109041.

[43] R.G. Parton and M.A. del Pozo, Caveolae as plasma membrane sensors, protectors and organizers, *Nat Rev Mol Cell Biol* **2**(14) (2013), 98–112.

[44] L. Bai, X. Deng, Q. Li, M. Wang, W. An, A. Deli et al., Down-regulation of the cavin family proteins in breast cancer, *J Cell Biochem* **1**(113) (2012), 322–8.

[45] J. Peng, H.Z. Liu, J. Zhong, Z.F. Deng, C.R. Tie, Q. Rao et al., MicroRNA187 is an independent prognostic factor in lung cancer and promotes lung cancer cell invasion via targeting of PTRF, *Oncol Rep* **5**(36) (2016), 2609–18.

[46] K. Yi, Q. Zhan, Q. Wang, Y. Tan, C. Fang, Y. Wang et al., PTRF/cavin-1 remodels phospholipid metabolism to promote tumor proliferation and suppress immune responses in glioblastoma by stabilizing cPLA2, *Neuro Oncol* **3**(23) (2021), 387–99.

[47] L. Liu, H.X. Xu, W.Q. Wang, C.T. Wu, T. Chen, Y. Qin et al., Cavin-1 is essential for the tumor-promoting effect of caveolin-1 and enhances its prognostic potency in pancreatic cancer, *Oncogene* **21**(33) (2014), 2728–36.

[48] J. Huertas-Martínez, F. Court, S. Rello-Varona, D. Herrero-Martín, O. Almacellas-Rabaiget, M. Sáinz-Jaspeado et al., DNA methylation profiling identifies PTRF/Cavin-1 as a novel tumor suppressor in Ewing sarcoma when co-expressed with caveolin-1, *Cancer Lett*, (386) (2017), 196–207.

[49] Y. Qiu, C. Pu, Y. Li and B. Qi, Construction of a circRNA-miRNA-mRNA network based on competitive endogenous RNA reveals the function of circRNAs in osteosarcoma, *Cancer Cell Int*, (20) (2020), 48.

[50] P. Jansa, S.W. Mason, U. Hoffmann-Rohrer and I. Grummt, Cloning and functional characterization of PTRF, a novel protein which induces dissociation of paused ternary transcription complexes, *Embo J* **10**(17) (1998), 2855–64.

[51] M.M. Hill, M. Bastiani, R. Luetterforst, M. Kirkham, A. Kirkham, S.J. Nixon, et al., PTRF-Cavin, a conserved cytoplasmic protein required for caveola formation and function, *Cell* **1**(132) (2008), 113–24.